

# Extracting $(n,\gamma)$ direct capture cross sections from Coulomb dissociation: application to $^{14}\text{C}(n,\gamma)^{15}\text{C}$

N. C. Summers<sup>1,2</sup> and F. M. Nunes<sup>2,3</sup>

<sup>1</sup>LLNL, P.O. Box 808, L-414, Livermore, California 94551

<sup>2</sup>National Superconducting Cyclotron Laboratory, Michigan State University, East Lansing, Michigan 48824

<sup>3</sup>Department of Physics and Astronomy, Michigan State University, East Lansing, Michigan 48824

(Dated: December 15, 2018)

A methodology for extracting neutron direct capture rates from Coulomb Dissociation data is developed and applied to the Coulomb dissociation of  $^{15}\text{C}$  on  $^{208}\text{Pb}$  at 68 MeV/nucleon. Full Continuum Discretized Coupled Channel calculations are performed and an asymptotic normalization coefficient is determined from a fit to the breakup data. Direct neutron capture calculations using the extracted asymptotic normalization coefficient provide  $(n,\gamma)$  cross sections consistent with direct measurements. Our results show that the Coulomb Dissociation data can be reliably used for extracting the cross section for  $^{14}\text{C}(n,\gamma)^{15}\text{C}$  if the appropriate reaction theory is used. The resulting error bars are of comparable magnitude to those from the direct measurement. This procedure can be used more generally to extract capture cross sections from breakup reactions whenever the desired capture process is fully peripheral.

PACS numbers: 21.10.Jx, 25.60.Gc, 25.60.Tv

*Introduction.* Neutron direct capture reactions can play an important role in a variety of astrophysical sites, including big bang, stellar environments, and supernovae. Often, at the relevant energies, these capture rates are extremely small, making the direct measurement very difficult. Presently, direct measurements of neutron captures on short lived unstable nuclei are not possible. The Coulomb dissociation method [1] provides an alternative option with different systematic errors and theoretical challenges. The aim of this work is to provide a methodical and reliable procedure to extract the desired  $(n,\gamma)$  cross section from intermediate energy Coulomb Dissociation data.

Here we consider the particular example of  $^{14}\text{C}(n,\gamma)^{15}\text{C}$ . This reaction is of interest to astrophysics for a variety of reasons: (i) it is the slowest in the neutron induced CNO cycle that takes places in AGB stars [2]; (ii) it has impact on the abundances of the heavy elements produced by non-homogeneous big bang models [3]; (iii) it modifies the abundances resulting from the r-process in massive Type II supernovae [4]. In addition, it is one of the few that has been repeatedly studied through Coulomb Dissociation and for which direct measurements exist.

Shortly after its astrophysical relevance was identified, a first measurement of  $^{14}\text{C}(n,\gamma)^{15}\text{C}$  was performed at Karlsruhe [5]. As the container surrounding the target had been strongly activated by a previous experiment, the measurement had to be repeated many years later [6] in order to obtain a reliable result. In the meantime, a number of Coulomb dissociation experiments have been performed using a  $^{15}\text{C}$  beam on a  $^{208}\text{Pb}$  target, at several beam energies: the lowest data is available at 35 MeV/nucleon [8], an intermediate energy measurement was performed at 68 MeV/nucleon [9] and a high energy experiment at 600 MeV/nucleon [10]. Meanwhile, another indirect method to obtain the  $(n,\gamma)$  rate based on

mirror symmetry [11] showed discrepancies between all three methods: the direct method, the indirect Coulomb dissociation method and the mirror symmetry method. Then recently, the new direct measurements by Reifarth were revised and published in a conference proceeding [7], which agreed with the Coulomb dissociation measurements from RIKEN [9] and the mirror symmetry results [11]. The discrepancy with the MSU data [8] still remained.

Due to the weak binding of the  $^{15}\text{C}$  ground state, and because there are no low lying resonances, the  $(n,\gamma)$  cross section is mainly determined through the E1 direct transition from an initial p-wave scattering state to the ground state, with a small branch to the only excited bound state [11]. It is well known that this dominant E1 transition is completely peripheral and thus essentially fixed by the asymptotic normalization coefficient (ANC) of  $\langle ^{14}\text{C} | ^{15}\text{C} \rangle$  [11]. The  $1/2^+$  ground state is a halo n- $^{14}\text{C}$  s-wave, and the  $5/2^+$  excited state is mostly d-wave. In both cases the relevant physics can be described by a single particle model. As the continuum is structureless below 1 MeV, the capture cross section in this low energy region is not very dependent on the details of the scattering potential chosen — such as the radius and diffuseness — but is strongly dependent on the ANC of the bound state wavefunction.

While the calculation of the neutron capture rate is straightforward, the Coulomb dissociation requires a reliable reaction model. All three Coulomb dissociation measurements were analyzed with the virtual photon method [13], which is based on a first-order Coulomb-only semiclassical theory [14]. In [8], the nuclear component was determined from the scaling of the breakup cross section on lighter targets, and subsequently subtracted from the total measured cross section. In [9], the nuclear was excluded through the selection of impact parameters larger than  $b > 30$  fm. Once a Coulomb only cross section

is obtained, the virtual photon method provides a simple proportionality relation to extract the desired  $(n, \gamma)$  cross section.

The continuum discretized coupled channel method (CDCC) [15] provides a non-perturbative framework in which to describe the breakup process, treating Coulomb and nuclear effects on the same footing. Multipole excitations are fully taken into account as well as final state interaction effects (e.g. [16]). Systematic studies of Coulomb dissociation for loosely bound systems on a variety of targets, spanning a range of beam energies, have shown that nuclear scaling is not always reliable and nuclear-Coulomb interference can be very large [17]. In that work it is suggested that, rather than *massaging* the data to obtain a *Coulomb only* cross section, CDCC be used as a standard tool to analyze the full measured dissociation data. In this frame of mind, one would start with a single particle structure model for the projectile  $^{15}\text{C} = n + ^{14}\text{C}$  and would adjust the parameters to obtain a good description of the breakup data. The reaction model then already takes into account nuclear and Coulomb effects in a coherent manner. That same potential model for the projectile which fits the breakup data would then provide the corresponding neutron capture cross section.

A potential model for the projectile describing the breakup cross sections is not unique. Indeed, as shown in [18], for loosely bound systems, even if the geometries differ significantly, it is essentially the ANC that determines the normalization of the breakup cross section. This is also true for the neutron capture cross section whenever it is completely peripheral, as in the case of  $^{14}\text{C}(n, \gamma)^{15}\text{C}$ . The use of ANCs in the analysis of peripheral reactions was first introduced for transfer processes [12]. In this work we propose to use the dissociation data to extract the ANC of  $^{15}\text{C}(\text{g.s.})$  and then obtain from it the neutron capture cross section. We concentrate on the breakup data at 68 MeV/nucleon first, to show the reliability of our proposed procedure, and then discuss difficulties in the analysis of the data at 35 MeV/nucleon. We do not include the 600 MeV/nucleon experiment in our studies since, at these energies, converged CDCC calculations are very computational intensive and, given that relativistic effects are too strong to be considered approximately, results would not be reliable. A study of the theoretical sources of uncertainty in the procedure will also be presented.

*Methodology.* In this work, we propose a procedure for extracting direct neutron capture rates for loosely bound systems from Coulomb dissociation, independent of the specifics for the experiments. It relies on the fact that both, the breakup cross section and the capture cross section are proportional to the square of the ANC. The method is applied to  $^{14}\text{C}(n, \gamma)^{15}\text{C}$  that has been measured directly but also through Coulomb dissociation.

Our starting point is a set of  $^{14}\text{C}+n$  potentials which span a range of ANCs. In Table I we compile some  $^{14}\text{C}+n$  potentials from the literature and add a few of our own,

$V_s$	$V_p$	$R_0$	$a$	$C_{s1/2}$	Ref.
65.19	68.52	1.1	0.5	1.254	
61.17	64.96	1.15	0.5	1.272	[10]
55.36	60.43	1.223	0.5	1.298	[19]
54.91	61.13	1.22	0.53	1.319	
54.23	61.65	1.22	0.56	1.342	
52.79	61.85	1.228	0.6	1.376	[24]

TABLE I:  $^{14}\text{C}+n$  potential parameters and calculated ANCs. The spin orbit depth was fixed at 5 MeV with the same radius and diffuseness as the central part.

all with changing geometries. The  $V_s$  potential strength is obtained from fitting the binding energy of the s-wave ground state of  $^{15}\text{C}$ . The same  $V_s$  reproduces well the  $^{15}\text{C}$  d-wave resonance. The  $V_p$  potential strength is obtained from the binding energy of the  $p_{3/2}$  neutrons in  $^{14}\text{C}$ .  $V_s$  ( $V_p$ ) is used to calculate the scattering states with even (odd) parity. For each of these single particle potentials, CDCC calculations for the breakup of  $^{15}\text{C}$  on  $^{208}\text{Pb}$  are performed. Both bound states are included and fully coupled in the calculation. The CDCC model space needed for convergence includes partial waves for the internal motion of the projectile up to  $l \leq 3$  and maximum  $^{14}\text{C}+n$  relative energy  $E_{\text{rel}} \leq 8$  MeV, with a fine discretization from 0 – 2 MeV to obtain higher accuracy in this region (the number of bins below 2 MeV in each partial wave is  $N_{s1/2} = 10, N_{p1/2} = 10, N_{p3/2} = 20, N_d = 8, N_f = 5$ ). For the projectile-target relative motion, the maximum partial wave included is  $L_{\text{max}} = 9000$ . The coupling potentials are expanded in multipoles and we include all multipolarities up to  $Q = 3$ . As to the radial truncations, energy bins are integrated out to 50 fm and the CDCC equations are solved up to  $R_{\text{max}} = 1000$  fm.

For each of the breakup energy distribution theoretical curves, the  $\chi^2$  for the data of [9] was calculated. The function  $\chi^2(C_{s1/2})$  is quadratic and from its minimum we determine the ANC  $C_0$ , with an error from  $\chi^2_{\text{min}} + 1$  [20]. Based on this range of ANCs, neutron capture cross sections are calculated with an error bar originating from the fit to the breakup data. The code FRESKO [21] is used for both the breakup and capture calculations.

In summary, the proposed procedure involves a few steps: (i) define a set of neutron single particle potentials that generate a range of ANCs; (ii) calculate the corresponding breakup energy distributions in CDCC; (iii) for each single particle potential, calculate the  $\chi^2$  to the breakup data and fix the ANC  $C_0$  by minimizing  $\chi^2$  relative to the ANC; (iv) determine the error  $\epsilon_{C_0}$  in  $C_0$  through  $\chi^2_{\text{min}} + 1$ ; (v) calculate the neutron capture cross section corresponding to  $C_0 \pm \epsilon_{C_0}$ .

There are a few details that can be a source of uncertainty to this procedure. As mentioned in the introduction, there is a nuclear contribution to the breakup reaction which is included in our CDCC calculations. Fragment-target optical potentials are usually fitted to elastic scattering to reduce the ambiguity. In this partic-

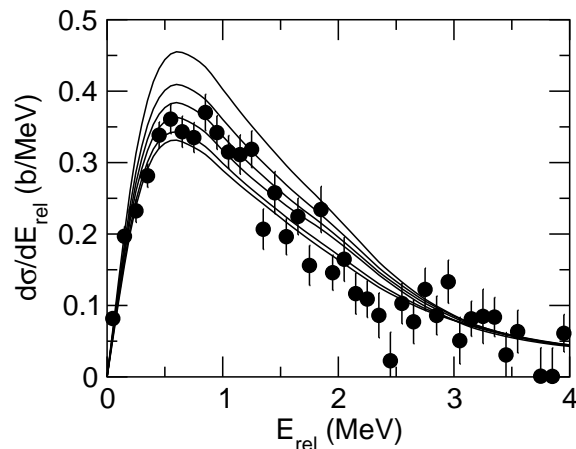


FIG. 1: Differential cross section with respect to energy for  $^{15}\text{C} \rightarrow ^{14}\text{C} + n$  breakup on  $^{208}\text{Pb}$ . The data are from Ref. [9] and the lines represent the cross sections obtained from each of the potential sets in Table I.

ular example we use the neutron optical potential from Perey and Perey [22] and the  $^{14}\text{C}$  optical potential was taken from  $^{10}\text{Be} + ^{208}\text{Pb}$  scattering, as in [23], with a mass scaled radius. It has been shown [24] that for the breakup of  $^{15}\text{C}$  on  $^{208}\text{Pb}$  at 68 MeV/nucleon, the sensitivity to details of these potentials is small.

Finally there is the issue of the single particle structure of the projectile. For other cases, the single particle approximation has been shown to carry a significant error [25]. As discussed in previous works (see for example [11] and Ref. within), the ground state of  $^{15}\text{C}$  is considered to be a very good single particle case with spectroscopic factor very close to  $S_{s_{1/2}} = 1$ . Even if this were not the case, when both the low energy capture and breakup are completely peripheral, the s-wave component dominates the cross section. This part is directly proportional to the bound state ANC, in such a way that the dependence on the single particle parameters and the spectroscopic factor is negligible once the ANC is fixed  $C_{g.s.}^2 = S_{s_{1/2}} b_{2s_{1/2}}^2$ . As mentioned above, in  $^{15}\text{C}$  there is also a d-wave excited state. The contribution of this state to the neutron capture is small and uncertainty in the structure of this state does not affect the errors bars.

**Results.** We present in Fig. 1 the results for the breakup cross sections of  $^{15}\text{C}$  on  $^{208}\text{Pb}$  at 68 MeV/nucleon, calculated within CDCC using the model space described in the previous section. The shape of the distribution compares well with the data. Most importantly, the peak of the cross section scales linearly with the the ANC-squared. For each of the theoretical curves,  $\chi^2$  was calculated and a quadratic relation with the ANC was determined. By minimizing the  $\chi^2$ , an ANC was fixed  $C_0 = 1.28 \pm 0.01 \text{ fm}^{-1/2}$ , the error bar corresponding to  $\chi_{\min}^2 + 1$ . These allowed ANC values produce a range of possible neutron capture cross sections, shown by the shaded area in Fig. 2.

Plotted in Fig. 2 is the range for  $\sigma_{n,\gamma} E^{-1/2}$  based on

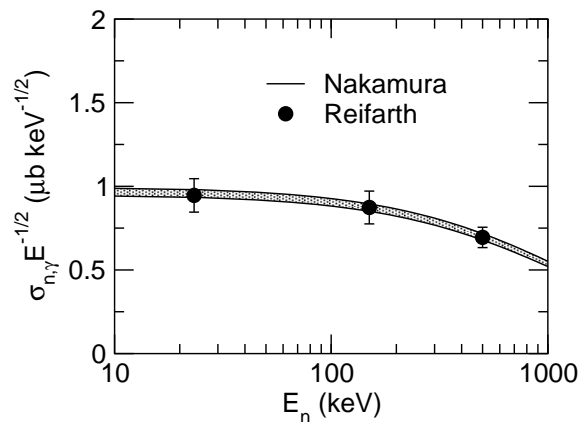


FIG. 2: Capture cross sections, multiplied by the energy factor  $E^{-1/2}$ , versus neutron energy. The shaded area are cross sections obtained from the RIKEN data [9] and the black circles are the latest direct measurements [7].

the RIKEN Coulomb dissociation data, compared with the data from the latest direct measurements [7]. The agreement is very good. Note that the lowest energy point in Fig. 2 at 23 keV does not correspond to a monoenergetic neutron measurement. The neutrons at this energy have a Maxwellian distribution, so an averaged cross section is obtained. For 23 keV too, the prediction based on the RIKEN Coulomb dissociation data ( $7.0 \pm 0.2 \mu\text{b}$ ) compares well with the direct measurement ( $7.1 \pm 0.5 \mu\text{b}$ ). For the purpose of the comparison in Fig. 2, we multiplied the 23 keV data point by 0.67, which is the factor one obtains assuming a perfect  $E^{-1/2}$  energy dependence in the cross section (valid at this low energy).

A lower energy breakup measurement is also available [8]. A direct comparison of theoretical cross sections with the experimental data was not possible for this experiment due to a non-linear energy response function of the detectors. Therefore the theoretical cross sections had to be folded with the detector efficiency in order to compare with the data. The analysis in Ref. [8] suggested an  $(n, \gamma)$  cross section approximately half that found in the analysis on the RIKEN data presented in the previous section and other direct and indirect measurements [6, 10, 11]. Here we present CDCC calculations which test the assumptions that appeared in the analysis of Ref. [8]. For the purpose of this study we use the single particle model of Ref. [19], with again the Perey-Perey [22] neutron-Pb potential and the same optical potential for the core as in the previous section.

The first important assumption in Ref. [8] is that the nuclear contribution can be subtracted from the data to leave a *Coulomb only* cross section. This was attempted by measuring the breakup data on a range of targets from the heavy Pb down to the light C target. Assumptions were made on how the Coulomb and nuclear cross sections scale with target mass, and by adding them incoherently, a least squares fit of the data was performed to estimate the relative cross sections so that the nuclear

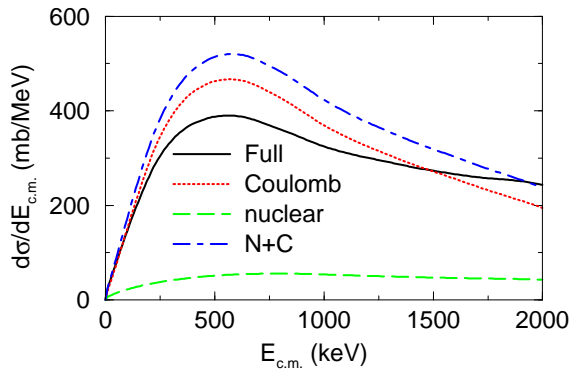


FIG. 3: (Color online) Nuclear and Coulomb interference in the Coulomb breakup of  $^{15}\text{C}$  at 35 MeV/nucleon.

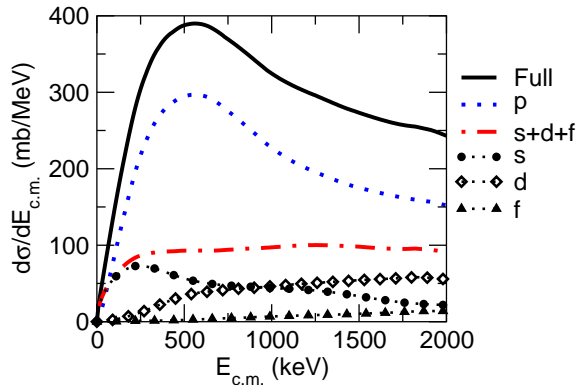


FIG. 4: (Color online) Partial wave decomposition of the cross section in the Coulomb breakup of  $^{15}\text{C}$  at 35 MeV/nucleon.

part could be subtracted.

In Fig. 3 we show the breakup energy distribution for the full calculation (solid line), including both nuclear and Coulomb, Coulomb only (dotted line), nuclear only (dashed line) and the incoherent sum of Coulomb and nuclear (dot-dashed line). The nuclear contribution is not negligible and interference effects are large, in agreement with the result of [17]. Most importantly, the shape of the distribution is changed when interference is taken into account. At low energies the full calculation including nuclear and Coulomb coherently is actually less than the Coulomb only calculation.

The other main assumptions appear in the analysis of the detector efficiencies. In order to calculate the efficiencies, a cross section must be entered into the Monte Carlo simulation of the detector response. The cross section used in Ref. [8] was obtained from first order perturbation theory. At this lower energy, the main assumptions of this theory over simplify the reaction mechanism, namely that the breakup proceeds via a single step E1 transition.

In our CDCC calculations we have included all multipoles up to  $Q = 3$  and  $^{14}\text{C}+n$  partial waves up to  $l \leq 3$ . In Fig. 4 we show the contribution of all the partial

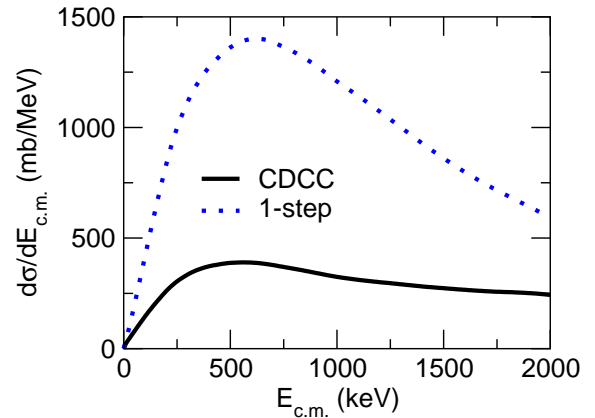


FIG. 5: (Color online) Higher-order effects in the Coulomb breakup of  $^{15}\text{C}$  at 35 MeV/nucleon.

waves. Although the p-wave is dominant (and is mainly E1 but would contain some nuclear contributions too), one should not neglect the other partial waves as it affects the normalization and the shape of the distribution.

In Fig. 5 we compare the full CDCC calculations with the corresponding one-step calculation. This corresponds to a DWBA calculation where the optical potentials used are the CDCC coupling potentials as discussed in [16]. It had already been shown [16] that multistep effects can be very large at energies close to the Coulomb barrier. Results presented in Fig. 5 show that at 35 MeV/nucleon multistep processes are also important and affect the normalization of the cross section.

These assumptions together overestimate the cross section used in the detector simulations, which in turn underestimate the efficiencies. Hence the theoretical cross sections which fit the data, once folded with the detector response functions come out much smaller than they should. This goes a long way to explaining why the capture cross sections derived from this data are approximately half that seen in other experiments. This outlines the need for good theoretical-experimental communication beyond the usual comparison at cross section level.

To summarize, in the analysis of [8] it was assumed that: (i) nuclear-Coulomb interference was insignificant; (ii) the outgoing neutrons were all in p-waves and (iii) the breakup process occurred in one-step. Given that these three assumptions are not correct, a re-analysis of this data would be highly desirable.

**Conclusions.** A procedure for determining the direct neutron capture reaction from intermediate Coulomb dissociation data is presented. The procedure is valid whenever the neutron capture is fully peripheral. Full CDCC calculations for the breakup process are compared to Coulomb dissociation data and a range of allowed asymptotic normalization coefficients is extracted from  $\chi^2$  minimization. Neutron capture cross sections consistent with this range of ANCs are determined.

The method is applied to  $^{14}\text{C}(n,\gamma)^{15}\text{C}$ . The Coulomb dissociation data of [9] is analyzed with CDCC and the

ANC  $C_0 = 1.28 \pm 0.01 \text{ fm}^{-1/2}$  is obtained for the  $^{15}\text{C}$  ground state. We show that the corresponding  $(n, \gamma)$  cross sections are consistent with direct measurements [7], providing comparable accuracy, and consistent with the results from mirror symmetry [11]. Previous discrepancies between all three methods were shown to be drastic in Ref. [11]. These discrepancies have been partially resolved by an improved analysis of the direct measurement by Reifarh *et al.* [7], with the exception of [8]. Our calculations imply that assumptions made in the analysis of Horváth *et al.* [8] are not valid. In order to include this measurement in the extraction of the  $^{14}\text{C}(n, \gamma)^{15}\text{C}$

cross section, a reanalysis of the data is needed.

We acknowledge valuable discussions with M. Heil and R. Cyburt, and T. Nakamura for providing the RIKEN Coulomb dissociation data. This work was partially supported by the Joint Institute for Nuclear Astrophysics at Michigan State University (N.S.F. grant PHY0216783), the National Science Foundation grant PHY-0555893, D.O.E grant DE-FG52-03NA00143 and in part performed under the auspices of the U.S. Department of Energy by Lawrence Livermore National Laboratory under Contract DE-AC52-07NA27344.

- 
- [1] G. Baur, C. A. Bertulani, and H. Rebel, Nucl. Phys. **A458**, 188 (1986).
  - [2] M. Wiescher, J. Gorres and H. Schatz, J. Phys. G **25**, R133 (1999).
  - [3] T. Kajino, G. J. Mathews and G. M. Fuller, Astrophys. J. **364**, 7 (1990).
  - [4] M. Terasawa *et al.*, Astrophys. J. **562**, 470 (2001).
  - [5] H. Beer *et al.*, Astrophys. J. **387**, 258 (1992).
  - [6] R. Reifarh *et al.*, Nucl. Phys. **A758**, 787c (2005).
  - [7] R. Reifarh *et al.*, Phys. Rev. C **77**, 015804 (2008) ; R. Reifarh *et al.* in proceedings of "Nuclei in the Cosmos - IX", CERN 2006, PoS(NIC-IX)223.
  - [8] Á. Horváth *et al.*, Astrophys. J. **570**, 926 (2002).
  - [9] T. Nakamura *et al.*, Nucl. Phys. **A722**, 301c (2003).
  - [10] U. D. Pramanik *et al.*, Phys. Lett. **551B**, 63 (2003).
  - [11] N. K. Timofeyuk, D. Baye, P. Descouvemont, R. Kamouni, and I. J. Thompson, Phys. Rev. Lett. **96**, 162501 (2006).
  - [12] H. M. Xu, *et al.*, Phys. Rev. Lett. **73**, 2027 (1994).
  - [13] C. Bertulani and G. Baur, Phys. Rep. **163**, 299 (1988).
  - [14] A. Winther and K. Alder, Nucl. Phys. **A319**, 518 (1979).
  - [15] M. Kamimura, M. Yahiro, Y. Iseri, H. Kameyama, Y. Sakuragi, and M. Kawai, Prog. Theor. Phys. Suppl. **89**, 1 (1986).
  - [16] F. M. Nunes and I. J. Thompson, Phys. Rev. C **59**, 2652 (1999).
  - [17] M. S. Hussein, R. Lichtenthäler, F. M. Nunes, and I. J. Thompson, Phys. Lett. **B640**, 91 (2006).
  - [18] P. Capel and F. M. Nunes, Phys. Rev. C **73**, 014615 (2006); Phys. Rev. C **75**, 054609 (2007).
  - [19] J. R. Terry *et al.*, Phys. Rev. C **69**, 054306 (2004).
  - [20] W.-M. Yao *et al.*, J. Phys. G **33**, 1 (2006).
  - [21] I. J. Thompson, Comput. Phys. Rep. **7**, 167 (1988).
  - [22] C. M. Perey and F. G. Perey, At. Data Nucl. Data Tables **17**, 1 (1976).
  - [23] N. Fukuda *et al.*, Phys. Rev. C **70**, 054606 (2004).
  - [24] P. Capel, D. Baye, and V. S. Melezhik, Phys. Rev. C **68**, 014612 (2003).
  - [25] N. C. Summers, F. M. Nunes and I. J. Thompson, Phys. Rev. C **73**, 031603(R) (2006); Phys. Rev. C **74**, 014606 (2006).